ISSN PRINT 2319 1775 Online 2320 7876

Research Paper © 2012 IJFANS. All Rights Reserved, UGC CARE Listed (Group -I) Journal Volume 11, Iss 11, 2022

# HYBRID AI APPROACH FOR LUNG CANCER DETECTION: SVM AND 3D CNN ANALYSIS FROM CT IMAGES

# Renikunta Ashok Kumar, Srinivas Nayini, B.Hema

Department of Computer Science Engineering, Sree Dattha Group of Institutions, Sheriguda, Hyderabad, Telangana

# **ABSTRACT**

Diagnostics for lung cancer in its early stages and therapy monitoring for lung cancer depend heavily on medical imaging technologies. For the purpose of detecting lung cancer, a number of medical imaging modalities, including computed tomography, magnetic resonance imaging, positron emission tomography, chest X-ray, and molecular imaging approaches, have been thoroughly examined. Some of the disadvantages of these systems include their inability to automatically categorize cancer images, making them inappropriate for use in patients with other illnesses. The development of a sensitive and precise method for the early diagnosis of lung cancer is desperately needed. One of the areas of medical imaging that is expanding the fastest is deep learning, with quickly developing applications involving textural and medical image-based data modalities. Medical imaging technologies based on deep learning can help clinicians identify and categorize lung nodules more rapidly and precisely. Consequently, the sophisticated CNN model modifications are implemented in this study for the purpose of detecting lung cancer from chest scan images. The suggested CNN model outperforms the state-of-the-art support vector machine (SVM) classifier in machine learning when it comes to accurately classifying benign and malignant, or normal and cancerous, tissues. Furthermore, the quality metrics obtained reveal the higher performance of the suggested deep CNN model in supporting the experts in an improved diagnosis.

**Keywords:** Lung Cancer Diagnostics, Deep Learning, Chest X-Ray, Magnetic Resonance Imaging,

# 1. INTRODUCTION

Lung cancer is the primary cause of cancer death worldwide, with 2.09 million new cases and 1.76 million people dying from lung cancer in 2018 [1]. Four case-controlled studies from Japan reported in the early 2000s that the combined use of chest radiographs and sputum cytology in screening was effective for reducing lung cancer mortality. In contrast, two randomized controlled trials conducted from 1980 to 1990 concluded that screening with chest radiographs was not effective in reducing mortality in lung cancer [2, 3]. Although the efficacy of chest radiographs in lung cancer screening remains controversial, chest radiographs are more cost-effective, easier to access, and deliver lower radiation dose compared with low dose computed tomography (CT). A further disadvantage of chest CT is excessive false positive (FP) results. It has been reported that 96% of nodules detected by low-dose CT screening are FPs, which commonly leads to unnecessary follow-up and invasive examinations. Chest radiography is inferior to chest CT in terms of sensitivity but superior in terms of specificity. Taking these characteristics into consideration, the development of a computer-aided diagnosis (CAD) model for chest radiograph would have value by improving sensitivity while maintaining low FP results [4].



ISSN PRINT 2319 1775 Online 2320 7876

Research Paper © 2012 IJFANS. All Rights Reserved, UGC CARE Listed ( Group -I) Journal Volume 11, Iss 11, 2022

Many computer-aided detection (CAD) systems have been extensively studied for lung cancer detection and classification [5, 6]. Compared to trained radiologists, CAD systems provide better lung nodules and cancer detection performance in medical images. Generally, the CAD-based lung cancer detection system includes four steps: image processing, extraction of the region of interest (ROI), feature selection, and classification. Among these steps, feature selection and classification play the most critical roles in improving the accuracy and sensitivity of the CAD system, which relies on image processing to capture reliable features. However, benign, and malignant nodule classification is a challenge. Therefore, a rapid, cost-effective, and highly sensitive deep learning-based CAD system for lung cancer prediction is urgently needed.

# 2. LITERATURE SURVEY

The development of malignant cells in the lungs is known as lung cancer. Overall men and women's mortality rates have increased as a result of growing cancer incidence. Lung cancer is a disease wherein the cells in the lungs quickly multiply. Lung cancer cannot be eradicated, but it can be reduced [7]. The number of people affected with lung cancer is precisely equal to the number of people who smoke continuously. Lung cancer treatment was evaluated using classification approaches such as Naive Bayes, SVM, Decision Tree, and Logistic Regression. Pradhan et al. [8] conduct an empirical evaluation of multiple machine learning methods that can be used to identify lung cancer using IoT devices. A survey of roughly 65 papers employing machine learning techniques to forecast various diseases was conducted in this study. The study focuses on a variety of machine learning methods for detecting a variety of diseases in order to identify a gap in prospective lung cancer detection in medical IoT. Deep residual learning is used by Bhatia et al. [9] to identify lung cancer from CT scans. With the UNet and ResNet algorithms, we propose a series of pre-processing approaches for emphasising cancer-prone lung regions and retrieving characteristics. The extracted features are fed through several classifiers, namely Adaboost and Random Forest, and the individual predictions are ensembled to calculate the likelihood of a CT scan becoming cancerous.

Without learning inadequate human information, Shin et al. [10, 11] use deep learning to investigate the characteristics of cell exosomes and determine the similarities in human plasma extracellular vesicles. The deep learning classifier was tested with exosome SERS data from regular and lung cancer cell lines and was able to categorise them with 95% efficiency. The deep learning algorithm projected that 90.7% of patients' plasma exosomes were more similar to lung cancer cell extracellular vesicles than the mean of healthy controls in 43 patients, encompassing stage I and II cancer patients. In the ability to forecast lung ADC subtypes, researchers looked at four clinical factors: age, sex, tumour size, and smoking status, as well as 40 radiomic markers. The LIFEx software was used to extract radiomic characteristics from PET scans of segmented cancers. The clinical and radio mic variables were ranked, and a subset of meaningful features was chosen based on Gini coefficient scores for histopathological class relationships [12]. In the estimation of survival, a deep learning network with a tumour cell and metastatic staging system was used to examine the dependability of individual therapy suggestions supplied by the deep learning preservation neural network. The C statistics were employed to evaluate the performance of the model. The computational intelligence survival



Research Paper © 2012 IJFANS. All Rights Reserved, UGC CARE Listed ( Group -I) Journal Volume 11, Iss 11, 2022

neural network model's longevity forecasts and treatment strategies were made easier with the use of a customer interface [13].

#### 3. PROPOSED METHODOLOGY

#### 3.1 Overview

A deep CNN model for lung cancer classification from CT scan images is a powerful approach that leverages the capabilities of deep learning to automatically learn and extract relevant features from raw image data. Here is an overview of how a deep CNN model can be used for classifying CT scan images into normal and malignant categories:

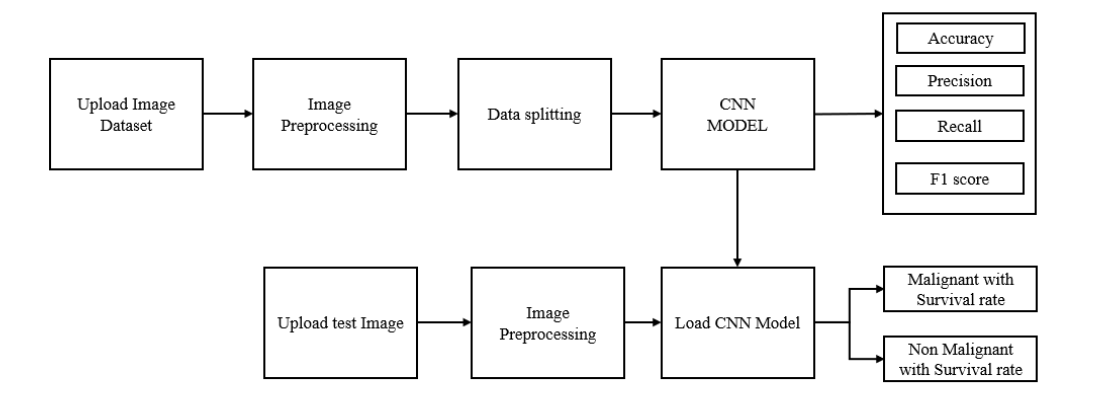


Figure 1: Block Diagram of Proposed Model

#### 3.2 CNN Basics

According to the facts, training and testing of proposed model involves in allowing every source image via a succession of convolution layers by a kernel or filter, rectified linear unit (ReLU), max pooling, fully connected layer and utilize SoftMax layer with classification layer to categorize the objects with probabilistic values ranging from [0,1]. Convolution layer as is the primary layer to extract the features from a source image and maintains the relationship between pixels by learning the features of image by employing tiny blocks of source data. It's a mathematical function which considers two inputs like source image I(x, y, d) where x and y denotes the spatial coordinates i.e., number of rows and columns. d is denoted as dimension of an image (here d = 3, since the source image is RGB) and a filter or kernel with similar size of input image and can be denoted as  $F(k_x, k_y, d)$ .

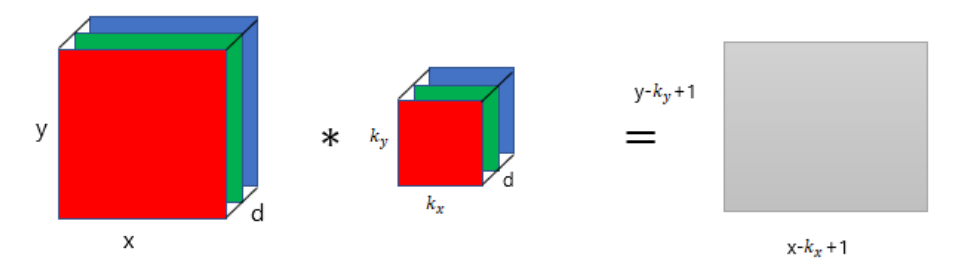


Fig. 2: Representation of convolution layer process.

The output obtained from convolution process of input image and filter has a size of  $C((x-k_x+1),(y-k_y+1),1)$ , which is referred as feature map. Let us assume an input



ISSN PRINT 2319 1775 Online 2320 7876

Research Paper © 2012 IJFANS. All Rights Reserved, UGC CARE Listed ( Group -I) Journal Volume 11, Iss 11, 2022

image with a size of  $5 \times 5$  and the filter having the size of  $3 \times 3$ . The feature map of input image is obtained by multiplying the input image values with the filter values.

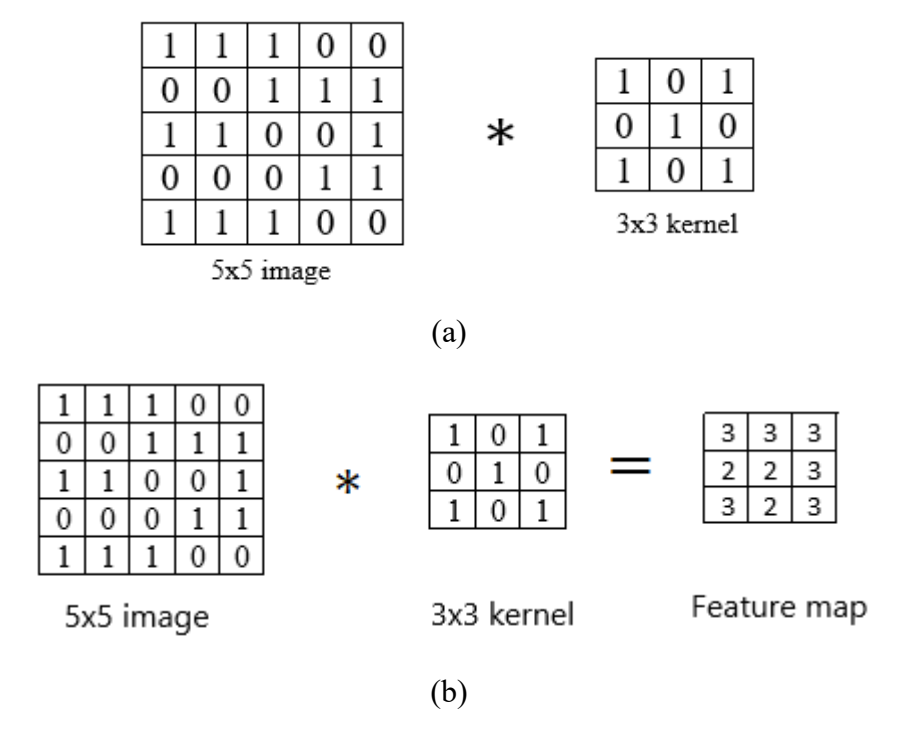


Fig. 3: Example of convolution layer process (a) an image with size  $\mathbf{5} \times \mathbf{5}$  is convolving with  $\mathbf{3} \times \mathbf{3}$  kernel (b) Convolved feature map

# 3.3.1 ReLU layer

Networks those utilizes the rectifier operation for the hidden layers are cited as rectified linear unit (ReLU). This ReLU function  $\mathcal{G}(\cdot)$  is a simple computation that returns the value given as input directly if the value of input is greater than zero else returns zero. This can be represented as mathematically using the function  $max(\cdot)$  over the set of 0 and the input x as follows:

$$G(x) = \max\{0, x\}$$

# 3.3.2 Max pooing layer

This layer mitigates the number of parameters when there are larger size images. This can be called as subsampling or down sampling that mitigates the dimensionality of every feature map by preserving the important information. Max pooling considers the maximum element form the rectified feature map.

# 3.3.3 Softmax classifier

Generally, as seen in the above picture softmax function is added at the end of the output since it is the place where the nodes are meet finally and thus, they can be classified. Here, X is the input of all the models and the layers between X and Y are the hidden layers and the data is passed from X to all the layers and Received by Y. Suppose, we have 10 classes, and we predict for which class the given input belongs to. So, for this what we do is allot each class with a particular predicted output. Which mean that we have 10 outputs corresponding to 10 different class and predict the class by the highest probability it has.



Research Paper © 2012 IJFANS. All Rights Reserved, UGC CARE Listed ( Group -I) Journal Volume 11, Iss 11, 2022

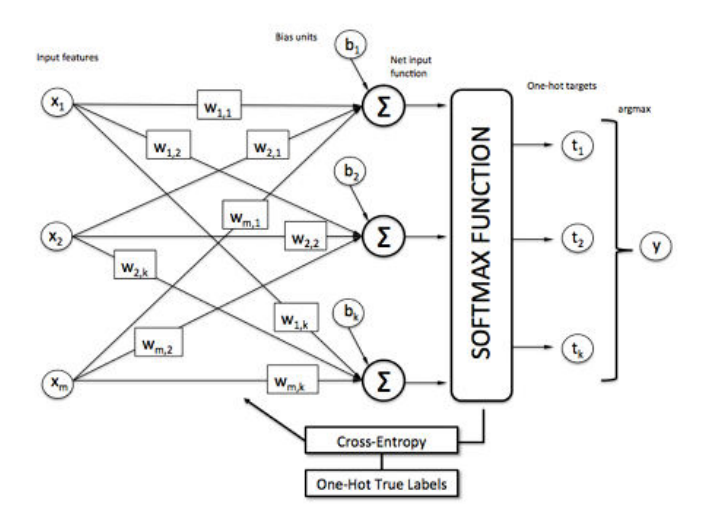


Fig.4: SoftMax classifier.

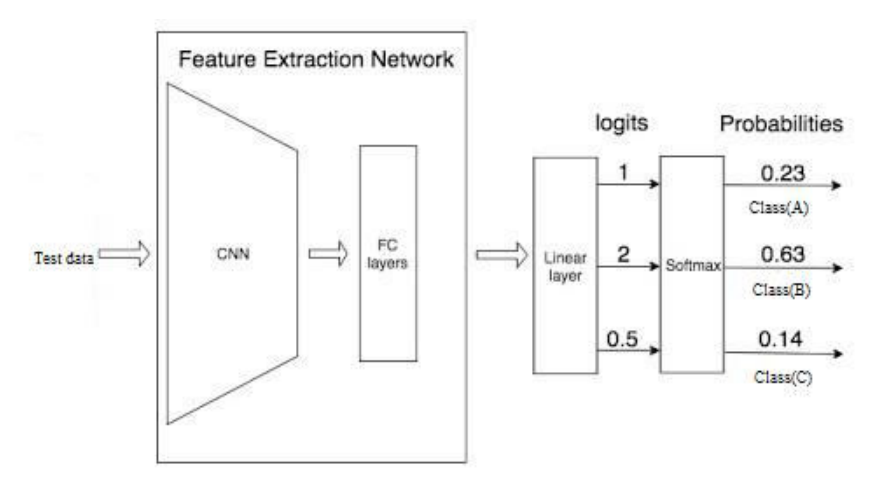


Fig.5: Example of SoftMax classifier.

In Figure 6, and we must predict what is the object that is present in the picture. In the normal case, we predict whether the lung is A. But in this case, we must predict what is the object that is present in the picture. This is the place where softmax comes in handy. As the model is already trained on some data. So, as soon as the picture is given, the model processes the pictures, send it to the hidden layers and then finally send to softmax for classifying the picture. The softmax uses a One-Hot encoding Technique to calculate the cross-entropy loss and get the max. One-Hot Encoding is the technique that is used to categorize the data. In the previous example, if softmax predicts that the object is class A then the One-Hot Encoding for:

Class A will be [1 0 0]

Class B will be [0 1 0]

Class C will be [0 0 1]

From the diagram, we see that the predictions are occurred. But generally, we don't know the predictions. But the machine must choose the correct predicted object. So, for machine to identify an object correctly, it uses a function called cross-entropy function.

So, we choose more similar value by using the below cross-entropy formula.



ISSN PRINT 2319 1775 Online 2320 7876

Research Paper © 2012 IJFANS. All Rights Reserved, UGC CARE Listed ( Group -I) Journal Volume 11, Iss 11, 2022

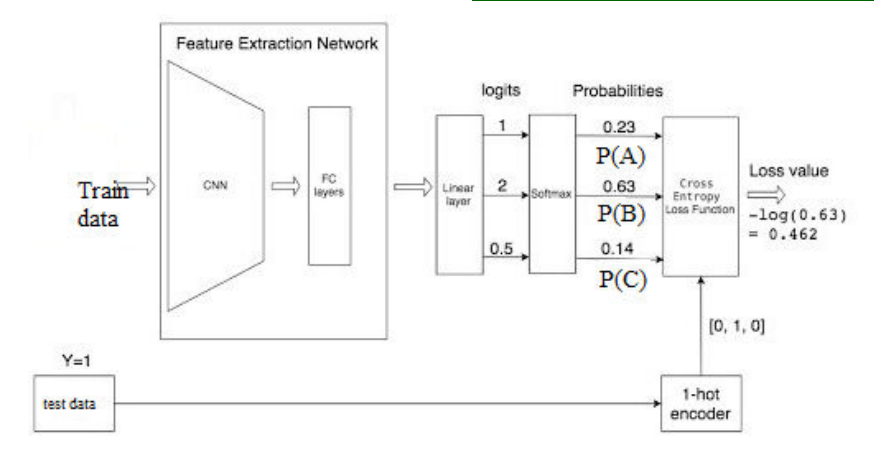


Fig.6: Example of SoftMax classifier with test data.

In the above example we see that 0.462 is the loss of the function for class specific classifier. In the same way, we find loss for remaining classifiers. The lowest the loss function, the better the prediction is. The mathematical representation for loss function can be represented as: -

$$LOSS = np.sum(-Y * np.log(Y\_pred))$$

### 4. RESULTS AND DISCUSSION

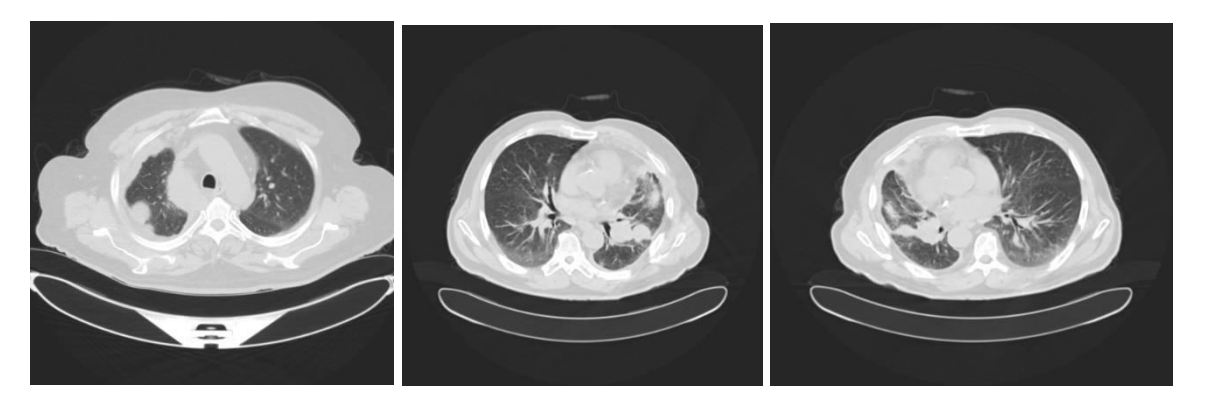


Figure 7: Sample images from dataset with Non-Malignant class.

Figure 7 shows that Presents a collection of images sourced from a dataset categorized as Non-Malignant class. Each image visibly represents lung tissue devoid of any cancerous manifestations, serving as representative samples for this class in the dataset. Figure 8 shows that Exhibits a series of images sourced from a dataset categorized as Malignant class. Each image conspicuously showcases lung tissue displaying cancerous growth or abnormalities, thereby serving as exemplars for this category within the dataset. Figure 9 shows Depicts the visual layout of a user interface (UI) tailored for the explicit purpose of detecting instances of lung cancer within images. This UI encompasses various interactive elements and functionalities aimed at facilitating the process of image-based lung cancer detection.



Research Paper © 2012 IJFANS. All Rights Reserved, UGC CARE Listed ( Group -I) Journal Volume 11, Iss 11, 2022

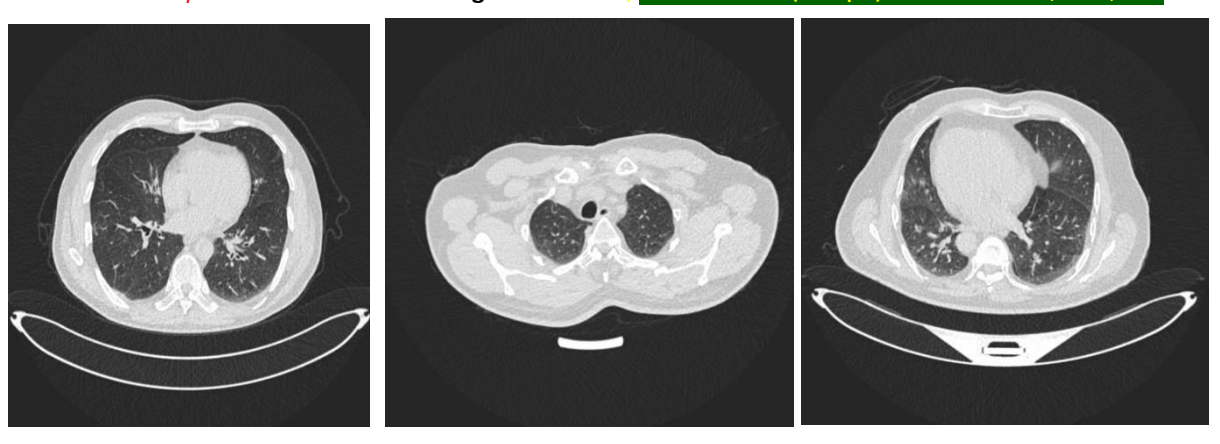


Figure 8: Sample images from dataset with Malignant class.



Figure 9: sample UI used for Lung cancer detection from images



Figure 10: UI shows the data after image preprocessing

Figure 10 shows Demonstrates the visual representation of data presented within the UI subsequent to undergoing a series of preprocessing steps. These preprocessing steps typically involve image enhancements, corrections, or feature extraction techniques aimed at optimizing the images for subsequent analysis and detection tasks. Figure 11 shows Illustrates the graphical depiction of the performance metrics attributed to a Support Vector Classifier (SVM) utilized for the task of lung cancer detection. These metrics may include accuracy, precision, recall, or F1-score, indicating the efficacy of the SVM model in distinguishing between cancerous and non-cancerous lung tissue. Figure 12: Exhibits a visual representation of the confusion matrix corresponding to the performance evaluation of the SVM Classifier. This confusion matrix offers a comprehensive breakdown of the classifier's predictive performance, including true positive, false positive, true negative, and false negative classifications.



Research Paper © 2012 IJFANS. All Rights Reserved, UGC CARE Listed ( Group -I) Journal Volume 11, Iss 11, 2022

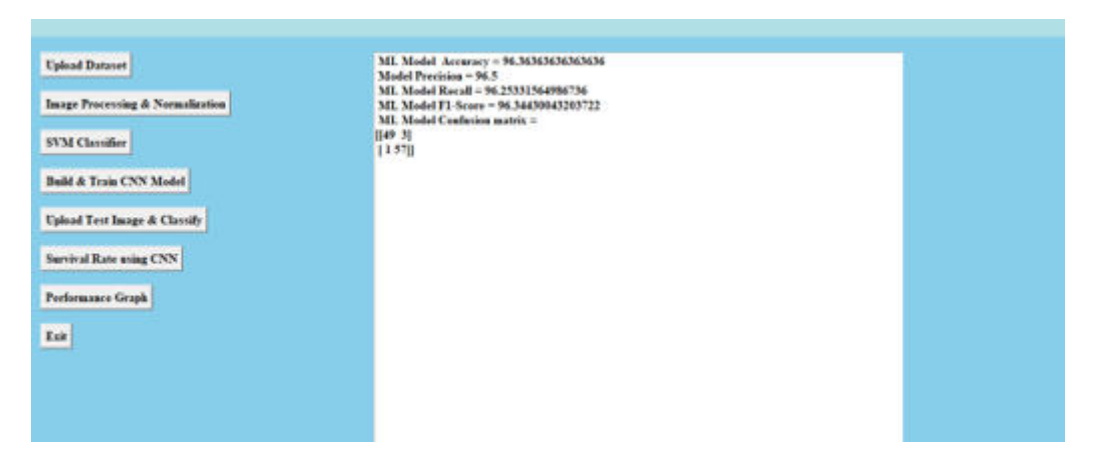


Figure 11: Performance of Support vector classifier

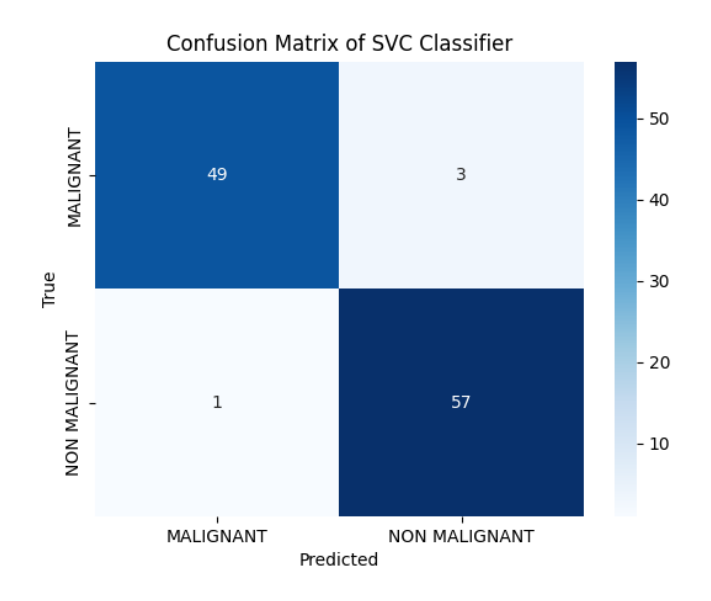


Figure 12: Confusion matrix of SVM Classifier

```
Uplead Dataset

CNN Model Accuracy = 100.0
CNN Model Precision matrix = 100.0
CNN Model Precision matrix = 100.0
CNN Model Carletion matrix =
```

Figure 13: Performance evaluation of CNN Classifier



Research Paper © 2012 IJFANS. All Rights Reserved, UGC CARE Listed (Group -I) Journal Volume 11, Iss 11, 2022

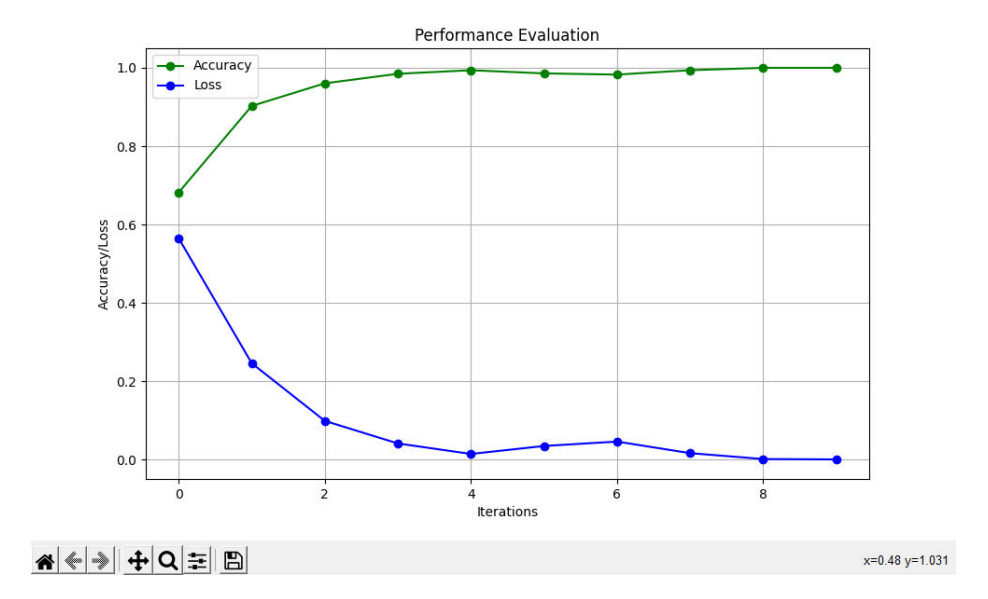


Figure 14: Iteration wise accuracy and loss graph

Figure 13 Showcases a graphical representation of the performance evaluation metrics associated with a Convolutional Neural Network (CNN) Classifier deployed for lung cancer detection. This visual display highlights the CNN model's effectiveness in accurately identifying lung cancer instances within images. Figure 14 shows Displays an iteration-wise graphical representation of the accuracy and loss values observed during the training process of the CNN Classifier. This graph offers insights into the model's learning progress and convergence towards optimal performance over successive training iterations. Figure 15 shows Portrays the visual depiction of the confusion matrix corresponding to the proposed CNN Model's performance evaluation. This confusion matrix furnishes detailed insights into the CNN model's classification accuracy and error rates across different classes.

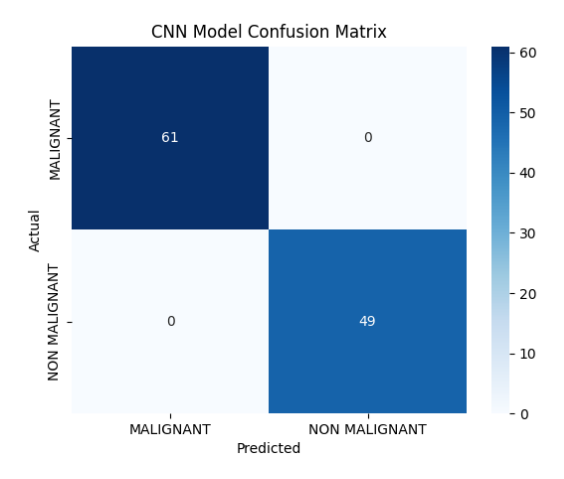


Figure 15: Confusion matrix of Proposed CNN Model



Research Paper © 2012 IJFANS. All Rights Reserved, UGC CARE Listed ( Group -I) Journal Volume 11, Iss 11, 2022

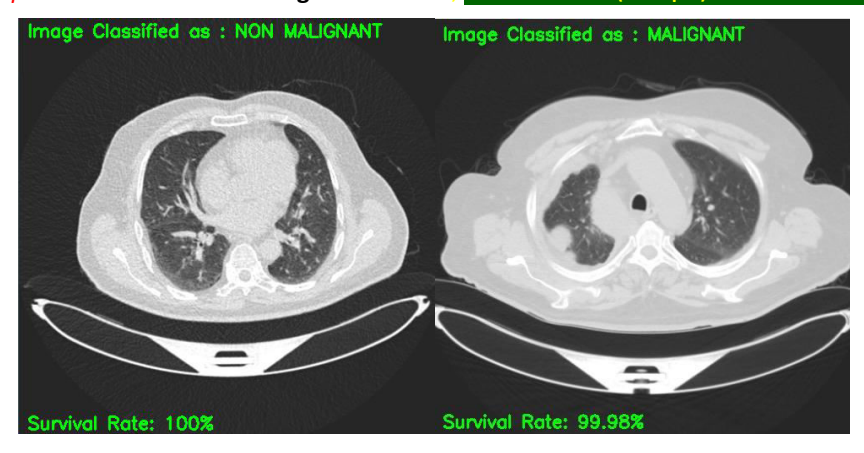


Figure 16: Prediction of survival rate and Prediction of output using CNN Model

Figure 16 shows Showcases the visual output generated by the CNN model, encompassing the predicted outcomes of lung cancer detection on a set of input images. This display likely includes examples of correctly and incorrectly classified lung tissue images. Figure 17 shows Consists of two distinct visual components; one representing the predictive estimation of survival rates based on detected lung cancer instances, and the other presenting the general output generated by the CNN Model. These visual outputs provide valuable insights into the prognostic capabilities and overall performance of the CNN model. Figure 18 shows that Presents a comparative graphical analysis between the performance metrics of the Gaussian Naïve Bayes (GNB) Classifier and the CNN Model. This comparative graph facilitates a comprehensive evaluation of the two models' respective effectiveness in lung cancer detection tasks

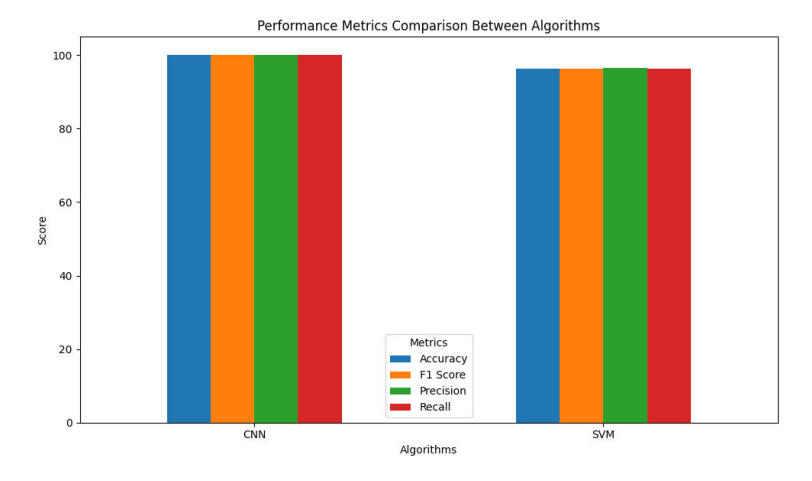


Figure 17: Performance Comparison graph of GNB Classifier and CNN Model.

#### 5. CONCLUSION

In conclusion, the implementation of advanced modifications in convolutional neural network (CNN) models for the detection of lung cancer from chest scan images represents a significant advancement in early-stage diagnosis and monitoring of lung cancer. The proposed CNN model exhibits superior performance in classifying benign and malignant cases, distinguishing between normal and cancerous conditions with higher accuracy compared to conventional machine learning approaches like support vector machine (SVM) classifiers. By harnessing the power of deep learning, clinicians can benefit from more accurate and efficient detection and



ISSN PRINT 2319 1775 Online 2320 7876

Research Paper © 2012 IJFANS. All Rights Reserved, UGC CARE Listed (Group -I) Journal Volume 11, Iss 11, 2022

classification of lung nodules, enabling earlier intervention and better patient outcomes. The incorporation of deep learning-based medical imaging tools into clinical practice enhances diagnostic capabilities and supports medical professionals in making informed decisions for patient care.

#### REFERENCES

- [1] Y. Xu, A. Hosny, R. Zeleznik, C. Parmar, T. Coroller, I. Franco, H.J. Aerts, Deep learning predicts lung cancer treatment response from serial medical imaging, Clin. Cancer Res. 25 (11) (2019) 3266–3275.
- [2] M.I. Faisal, S. Bashir, Z.S. Khan, F.H. Khan, An evaluation of machine learning classifiers and ensembles for early stage prediction of lung cancer, December, in: 2018 3rd International Conference on Emerging Trends in Engineering, Sciences and Technology (ICEEST), IEEE, 2018, pp. 1–4.
- [3] N. Coudray, P.S. Ocampo, T. Sakellaropoulos, N. Narula, M. Snuderl, D. Feny"o, A. Tsirigos, Classification and mutation prediction from non–small cell lung cancer histopathology images using deep learning, Nat. Med. 24 (10) (2018) 1559–1567.
- [4] D.M. Ibrahim, N.M. Elshennawy, A.M. Sarhan, Deep-chest: multi-classification deep learning model for diagnosing COVID-19, pneumonia, and lung cancer chest diseases, Comput. Biol. Med. 132 (2021), 104348.
- [5] Avanzo, J. Stancanello, G. Pirrone, G. Sartor, Radiomics and deep learning in lung cancer, Strahlenther. Onkol. 196 (10) (2020) 879–887.
- [6] S.H. Hyun, M.S. Ahn, Y.W. Koh, S.J. Lee, A machine-learning approach using PET-based radiomics to predict the histological subtypes of lung cancer, Clin. Nucl. Med. 44 (12) (2019) 956–960.
- [7] P. R. Radhika, R.A. Nair, G. Veena, A comparative study of lung cancer detection using machine learning algorithms, 2019, February, in: IEEE International Conference on Electrical, Computer and Communication Technologies (ICECCT), IEEE, 2019, pp. 1–4.
- [8] K. Pradhan, P. Chawla, Medical Internet of things using machine learning algorithms for lung cancer detection, J. Manag. Anal. 7 (4) (2020) 591–623.
- [9] S. Bhatia, Y. Sinha, L. Goel, Lung cancer detection: a deep learning approach, in: Soft Computing for Problem Solving, Springer, Singapore, 2019, pp. 699–705.
- [10] H. Shin, S. Oh, S. Hong, M. Kang, D. Kang, Y.G. Ji, Y. Choi, Early-stage lung cancer diagnosis by deep learning-based spectroscopic analysis of circulating exosomes, ACS Nano 14 (5) (2020) 5435–5444.
- [11] V. Rajasekar, B. Predi'c, M. Saracevic, M. Elhoseny, D. Karabasevic, D. Stanujkic, P. Jayapaul, Enhanced multimodal biometric recognition approach for smart cities based on an optimized fuzzy genetic algorithm, Sci. Rep. 12 (1) (2022) 1–11.
- [12] S.H. Hyun, M.S. Ahn, Y.W. Koh, S.J. Lee, A machine-learning approach using PET-based radiomics to predict the histological subtypes of lung cancer, Clin. Nucl. Med. 44 (12) (2019) 956–960.
- [13] Y. She, Z. Jin, J. Wu, J. Deng, L. Zhang, H. Su, C. Chen, Development and validation of a deep learning model for non–small cell lung cancer survival, JAMA Netw. Open 3 (6) (2020) e205842, e205842.

